Rapid aggregation and assembly in aqueous solution of Aβ (25-35) peptide

Lia Millucci[1], Roberto Raggiaschi[2], Davide Franceschini[2], Georg Terstappen[2] and Annalisa Santucci[1,*]

[1]*Department of Molecular Biology, University of Siena*
[2]*SienaBiotech, via Fiorentina 1, 53100 Siena, Italy*

**Corresponding author (Fax, +390577234903; Email, santucci@unisi.it)*

The highly toxic Aβ(25-35) is a peculiar peptide that differs from all the other commonly studied β-amyloid peptides because of its extremely rapid aggregation properties and enhanced neurotoxicity. We investigated Aβ(25-35) aggregation in H_2O at pH 3.0 and at pH 7.4 by means of in-solution analyses. Adopting UV spectroscopy, Congo red spectrophotometry and thioflavin T fluorimetry, we were able to quantify, in water, the very fast assembling time necessary for Aβ(25-35) to form stable insoluble aggregates and their ability to seed or not seed fibril growth. Our quantitative results, which confirm a very rapid assembly leading to stable insoluble aggregates of Aβ(25-35) only when incubated at pH 7.4, might be helpful for designing novel aggregation inhibitors and to shed light on the *in vivo* environment in which fibril formation takes place.

[Millucci L, Raggiaschi R, Franceschini D, Terstappen G and Santucci A 2009 Rapid aggregation and assembly in aqueous solution of Aβ (25-35) peptide; *J. Biosci.* **34** 293–303]

1. Introduction

Several laboratories have reported that, after being processed from its precursor protein, β-amyloid changes its conformation to form aggregates, which are eventually deposited as senile plaques, one of the key pathological hallmarks of Alzheimer disease (AD). One of the main theories of the causes of neurodegeneration in AD postulates that the production of β-amyloid (1-40) and (1-42) peptides causes the activation of a biochemical cascade that leads to cell death (Hölscher 2005). Nevertheless, the neurodegenerative effects of β-amyloid have not been shown consistently in cell culture or *in vivo* studies. In cell culture studies, cytotoxic effects can be observed under certain conditions but these are not always consistent (Hölscher 2005), and *in vivo* studies have shown that while infusion of β-amyloid has effects on behaviour, it does not necessarily induce neurodegenerative effects. The effects on memory formation and cognitive abilities due to injection of amyloid fragments into the brain have been very inconsistent until now. It has been proposed that the aggregation state of amyloid fragments is of crucial importance for inducing toxic effects. While low molecular aggregates display low toxicity, certain oligomers appear to be much more toxic than others (Walsh and Selkoe 2004), but it is not clear whether or how exactly infused soluble amyloid fragments aggregate in the brain (Holscher *et al.* 2007). Likewise, the correlation between neurotoxicity, structural properties and evolution of Aβ aggregates over time has not been completely understood. Based on these findings, intense effort has been focused on discovering a way to describe this aggregation process. As a result of the complexity and enormous structural space required even in relatively short 30–40 amino acid polypeptides, determining the molecular basis of the recognition and assembly processes fostering amyloid-fibril formation is a very complicated task. Moreover, the synthesis of large

Keywords. Aβ(25-35); aggregation; amyloid; assembly; seeding

Abbreviations used: AD, Alzheimer disease; DMSO, dimethyl sulphoxide; HFIP, hexafluorisopropanol; IBM, inclusion body myositis; NCC, nucleated conformational conversion'; OD, optical density; PBS, phosphate buffered saline; pI, isoelectric point; SDS, sodium dodecyl sulphate; TFA, trifluoroacetic acid; Th-T, thioflavin-T

peptides, especially aggregative peptides, is expensive and difficult. Consequently, an important direction for studying amyloid formation has emerged from the use of residues of peptide fragments (Gazit 2005).

The fibrillisation process of many synthetic amyloid peptides has been studied and the relative assembly dynamics have been found to be quite different (Petkova *et al.* 2005; Roychaudhuri *et al.* 2008; Snyder *et al.* 1994), providing extensive evidence for the effect of various parameters on *β*-amyloid fibrillisation. On the other hand, little is known about the toxicity related to these different aggregation mechanisms.

Various synthetic A*β*s form filamentous, *β*-sheet assemblies *in vitro* (Meinke and Hansmann 2007). Mounting evidence originating from *in vitro* toxicity studies with synthetic A*β* peptides shows that A*β*, in an aggregated state (fibril, protofibril, low molecular-weight oligomer, or diffusible, non-fibrillar ligand), is toxic to neurons in cultures (Bieschke *et al.* 2008; Stefani 2007; Baglioni *et al.* 2006; Dobson 2006). The assembly phenomenon is reported to be dependent on the pH of solutions, concentration of A*β*s and incubation time in solution (Wei and Shea 2006; Wang *et al.* 2004). Several *β*-amyloid fragments have been reported to form such assemblies, but only A*β*s that include a substantial portion of the transmembrane sequence were showed to be able to assemble into aggregates that are stable at pH 7.4 and resistant to disruption by sodium dodecylsulphate (SDS) (Burdick *et al.* 1992; Pike *et al.* 1993, 1995).

It has been suggested that the kind of solvent used to dissolve lyophilised A*β* peptides determines not only the initial conformation of A*β* but also the aggregation kinetic behaviour that follows (Wei and Shea 2006). Various dissolving systems including dimethyl sulphoxide (DMSO), H_2O, trifluoroacetic acid (TFA), phosphate buffered saline (PBS) and hexafluoroisopropanol (HFIP) have been utilised in a variety of studies associated with the most commonly used synthetic model peptides, A*β*(1-40) and A*β*(1-42), and with a number of partial fragments, all forming amyloid-like fibrils and similar aggregated structures (Bitan and Teplow 2005: LeVine 2004). However, the weak correlation among kinetic data that frequently differ, depending on the specific A*β* fragment being examined, is still a problem (Simmons *et al.* 1994). Despite the large number of studies on neurotoxicity and fibril morphology typical of each A*β* fragment, relatively few kinetic studies describe the behaviour of some of these molecules in solution. In particular, the initial stages of assembly of A*β*(25-35), containing the functional domain – sequence GSNKGAIIGLM – of the A*β* precursor protein that is required both for neurotrophic effects in normal neural tissues and is involved in the neurotoxic effects in AD, are difficult to monitor (Clementi *et al.* 2005; Jayaraman *et al.* 2008). Previous studies to evaluate the structure–activity requirements for age-dependent aggregation and neurotoxicity further revealed that peptides containing the hydrophobic A*β*(29-35) region slowly formed stable aggregates in solution even at pH 7.4 and were neurotoxic to neural cultures upon ageing but not in freshly prepared solution (Pike *et al.* 1993). The only and most notable exception to this age-dependent toxicity is A*β*(25-35) that is neurotoxic immediately upon dissolution (Takadera *et al.* 1993; Ban 2008). A*β*(25-35) is the shortest peptide sequence that retains biological activity comparable with that of full-length A*β*(1-42) and exhibits large *β*-sheet aggregated structures (Pike *et al*. 1995; D'Ursi *et al*. 2004). Moreover, A*β*(25-35) peptide is present in senile plaques and degenerating hippocampal neurons in AD brains, but not in age-matched control subjects. Certain forms of A*β*(1-40) can be converted to A*β*(25-35) peptide by brain proteases (Kubo *et al.* 2002). Finally, this proteolytic fragment of A*β*(1-40) was also observed in inclusion body myositis (IBM), a disorder known for the accumulation of proteins with amyloid characteristics in muscle (Jayaraman *et al.* 2008). Because of these features, A*β*(25-35) has often been chosen as a model for full-length A*β* in structural and functional studies but, unfortunately, kinetic and structural studies of this peptide are indeed strongly hampered by its tendency to quickly assemble into insoluble aggregates (Clementi *et al.* 2005; Misiti *et al.* 2005). On the other hand, the study of the conformational preferences of A*β*(25-35) in different conditions appears to be crucial for shedding light on its intrinsic structural properties related to A*β* fibril formation.

The data presented here more clearly define the uncommon rapidity with which A*β*(25-35) self-assembles at different pH and support the hypothesis that the early aggregated forms of A*β*(25-35) that develop at pH 3 may not enhance the growth of dangerous fibrils generated at pH 7.4.

We conclude from these data that the mechanism by which A*β* forms toxic fibrils is initiated *in vivo* and probably does not involve low pH compartments, confirming the hypothesis of Kubo *et al.* (2002) on the origin and peculiar toxicity of the A*β*(25-35) undecapeptide.

2. Materials and methods

2.1 *Peptides*

Synthetic A*β*(25-35) and A*β*(1-42) were purchased from Bachem (Torrance, CA, USA).

2.2 *Preparation of A*β *solutions*

2.2.1 *Unseeded conditions*: Samples of 1 mg of A*β*(25-35) were dissolved in 0.2 ml of TFA and gently stirred at 5°C

for 3 h to completely dissolve associated peptides (Carrotta *et al.* 2005). Upon addition of 1.8 ml of Millipore SuperQ water, solutions were fractionated into five equal parts and lyophilised overnight. This procedure provided stock powder aliquots of the same amount (200 μg). Each aliquot was dissolved in 250 μl of 0.1 M sodium citrate buffer at pH 3 or in water pH 7.4 and filtered (via a 0.2 μm Millipore filter) into 1 cm square quartz cuvettes. Different peptide concentrations were obtained by diluting the stock powder aliquots with a different amount of buffer solution. All chemicals were of reagent grade. *In vitro* experiments were performed in extremely simplified conditions to highlight a few basic features of the molecular interactions and mechanisms that drive amyloid fibrillogenesis.

2.2.2 *Seeded conditions:* Samples of 1 mg of Aβ(25-35) were dissolved in 2 ml of Millipore SuperQ water; solutions were fractionated into five equal parts and lyophilised overnight. Each aliquot was dissolved in a different amount of 0.1 M sodium citrate buffer at pH 3 or in water pH 7.4 to achieve the needed concentration. Aβ stock suspensions were immediately utilised for spectrophotometrical assay due to the tendency of Aβ(25-35) to aggregate in water also during freezing (data not shown). The seeding efficiency of the Aβ(25-35) aggregates was tested by introducing in the reaction mixture of unseeded peptide 10% (w/w) of aggregated Aβ(25-35) from a solution at pH 3.0 or 7.4, respectively.

2.3 *Verification of seed-free condition*

Pretreatment with TFA and filtering ensured that no large aggregates (seeds) were present in the solution (Carrotta *et al.* 2005). The high reproducibility of our kinetics in unseeded conditions further confirmed the absence of a significant amount of spurious nucleation seeds within our peptide solutions, before and after filtering.

2.4 *Turbidimetric assay*

For turbidity measurements, samples were prepared and, following incubation, absorbance was measured using an Agilent 8453 UV spectrophotometer set at a wavelength of 403 nm.

2.5 *UV spectroscopy (OD_{220} assay)*

We adopted a modified procedure described by Yoshiike *et al.* (2001). Aβ-stock solutions were first diluted in 20 mM Tris-HCl (pH 7.4 or pH 3) and centrifuged (Optima L90-K Ultracentrifuge) at 10 000 *g* for 10 min at 4°C. The supernatant containing soluble Aβ was mixed with the same volume of Tris buffer alone.

The concentration of Aβ in each test sample was 10 μM. At this point, each sample was divided into two equal volumes:

(i) one volume was diluted 10 times with buffer and termed 'before', and

(ii) the remaining volume was incubated for 30 min at 37°C and termed 'after'. At this point, to assess Aβ concentration, the optical density (OD) due to aggregation was calculated as the ratio of the difference between OD_{before} and OD_{after} divided by OD_{before} as follows:

$$(OD_{before} - OD_{after}) / OD_{before} \times 100\%$$

OD of the 'before' samples (OD_{before}) was measured using an Agilent 8453 UV spectrophotometer set at a wavelength of 220 nm.

After 30 min the 'after' samples were ultracentrifuged at 100 000 *g* for 10 min at 4°C using an Optima L90-K Ultracentrifuge.

Supernatants were collected, diluted 10 times with buffer, and absorbance was measured (OD_{after}) as described above. The percentage of total aggregation was calculated as described above.

Furthermore, the sedimentable portion of Aβ(25-35) solutions was quantified using the centrifugation protocol outlined below. Due to an inability to iodinate the Aβ(25-35) amyloid peptide using standard procedures, sedimentation of these peptides was quantified using Lowry protein determination (Bradford 1976). To accommodate the limitations of this assay, stock solutions were diluted to 25 μM in H_2O (pH 7.4 or pH 3) and centrifuged (Optima L90-K Ultracentrifuge) at 100 000 *g* for 1 h. The pellet and supernatant fractions were separated and protein concentration was determined. Percentage sedimentation was calculated as:

$$\frac{\sum_{n}\left(\frac{\text{protein conc.}\,Pellet}{\text{protein conc.}\,Pellet + \text{protein conc.}\,Supernatant}\right)\times 100}{n}$$

where *n* represents the number of observations.

2.6 *Congo red spectrophotometric assay*

2.6.1 *Congo red preparation:* A 100–300 mM stock solution of Congo red (CR) (CI 22120, Direct Red 28; Aldrich, Milwaukee, WI, USA) was prepared in filtered PBS (PBS: 0.01 M phosphate buffer, 0.0027 M KCl and 0.137 M NaCl, pH 7.4). To the CR stock solution 1% sodium azide was added to prevent the formation of microaggregates or other kinds of pollutants.

2.6.2 *CR binding assays:* CR–Aβ binding studies were conducted using a protocol modified from Klunk *et al.* (1998). Spectrophotometric analysis of CR–Aβ binding was performed using an Agilent 8453 spectrophotometer; all measurements were taken in wavelength-scanning mode (300–700 nm), using PBS as reference. Mixtures of CR and Aβ(25-35) were incubated at room temperature for 15 min prior to spectral analysis. Separate kinetic studies showed that the absorbance of the CR–Aβ complex reached a maximum by 6 min. Absorbance spectra from 300 to 700 nm were recorded for the CR–Aβ mixture as well as CR and Aβ alone at the appropriate concentrations. These spectra were used to determine the wavelength of a 'shoulder peak' of the CR–Aβ complex.

Finally, different concentrations of Aβ(25-35), seeded or under seed-free conditions, were mixed with a solution of CR in PBS to yield a final CR concentration of 20 μM. After zeroing in on PBS, the absorbance of all samples at 541 nm was recorded until stoppage of aggregation was demonstrated by CR-coloured large Aβ(25-35) macro-aggregates, easily visible to the naked eye.

2.7 *Thioflavin-T fluorescence spectroscopy assay*

Aggregate formation of Aβ was measured by a thioflavin-T (Th-T) fluorimetric assay (LeVine 1997) with a few modifications. Th-T binds specifically to amyloid, and this binding produces a shift in its emission spectrum and a fluorescent signal proportional to the quantity of amyloid formed. This method is more specific than others, such as turbidity or sedimentation assays, for the semiquantitative determination of amyloid-like aggregates. A seeded solution of Aβ(25-35) or Aβ(1-42) peptides in H_2O (pH 7.4) at different concentrations was added to 5.0 μM Th-T in a final volume of 3.0 ml of 50 mM Tris-HCl (pH 7.4). Fluorescence was monitored at excitation 440 nm and emission 482 nm using an RF-1500 spectrofluorometer (Shimadzu, Kyoto, Japan). A time scan of fluorescence was performed and, in each case, the fluorescence was normalised by subtracting the blank sample. The data from three identical samples in separate experiments were then averaged to provide the final values.

3. Results

Aβ(25-35) differs from other amyloid peptides due to its dramatically fast tendency to self-assemble and form insoluble aggregates. Until now, this property was the cause of the lack of accurate data pertaining to the aggregation kinetics of this peptide, and limited the study of its accentuated and precocious neurotoxicity (Maurice *et al.* 1996). To investigate the relationships among the conditions that promote rapid assembly of Aβ(25-35), the solubility properties of its aggregated forms and the real correspondence between properties of aggregates generated by both Aβ(25-35) and Aβ(1-42), we report a study of the aggregates formed by Aβ(25-35) at acidic pH compared with those formed at pH 7.4. Unlike Aβ(1-40), whose different aggregation properties at pH values of 5.8 and 7.4 were reported by Wood *et al.* (1996), Aβ(25-35) does not show any variation in aggregation ability if incubated at these pH values. We were able to observe discrepancies in aggregation kinetics, and peculiarities of the formed aggregates only at pH 3.0. We showed that Aβ(25-35) generates a turbid product, CR-binding aggregation reaction, within a few minutes when incubated in seeded conditions at both acidic and physiological pH. At pH 7.4 and unseeded conditions, Aβ(25-35) forms little or no aggregate in this time frame, requiring hours to complete fibril formation and the solution stays transparent. Otherwise, at pH 3.0, Aβ(25-35) seems to be a mixture of amorphous particles and, in contrast to fibrils grown at pH 7.4, the turbid aggregate generated at pH 3.0 is incapable of seeding fibril growth at pH 7.4.

We exclusively adopted in-solution techniques, since it has been well established in our laboratory as well as in others (Burdick *et al.* 1992; Pike *et al.* 1995) that Aβ(25-35) is the only β-amyloid fragment that cannot be analysed by electrophoretic techniques. We determined the time course of Aβ(25-35) aggregation and its assembly and sedimentation capacity at a percentage significantly higher than most other common β-peptides such as Aβ(1-40) and Aβ(1-42). We especially emphasise the discrepancies between Aβ(1-40) (Wood *et al.* 1996) and its proteolytic fragment Aβ(25-35) in forming aggregates at different pH values with different seeding properties.

Because it was postulated that fibril formation might be initiated in a low pH environment of the lysosome and there are reports in the literature of a pH optimum for Aβ(1-40) and Aβ(1-42) aggregation in the pH 5–6 range (Nesgaard *et al.* 2009), we report here the peculiar case of Aβ(25-35). This particular peptide aggregates in the same way at pH 7.4 and at pH 5.8 (data not shown), but we observed rapid formation of aggregates if incubated at pH 3. Once formed, the aggregates generated at pH 7.4 were relatively stable and resisted interconversion in response to a shift in pH. Figure 1 C, D shows that, as measured by turbidity, aggregates generated at pH 7.4 do not change significantly in character after a shift to another pH. In contrast, aggregates generated at pH 3.0 partially reduce their turbidity if shifted to pH 7.4.

The tendency of Aβ(25-35) to aggregate in H_2O was confirmed by evaluation of its percentage of aggregation and sedimentation (figure 1A, B). Congruently with aggregation quantification, Aβ(25-35) showed the highest sedimentation percentage (54%) with respect to the reference Aβ peptide. Although Pike *et al.* (1993) hypothesised, on the basis of

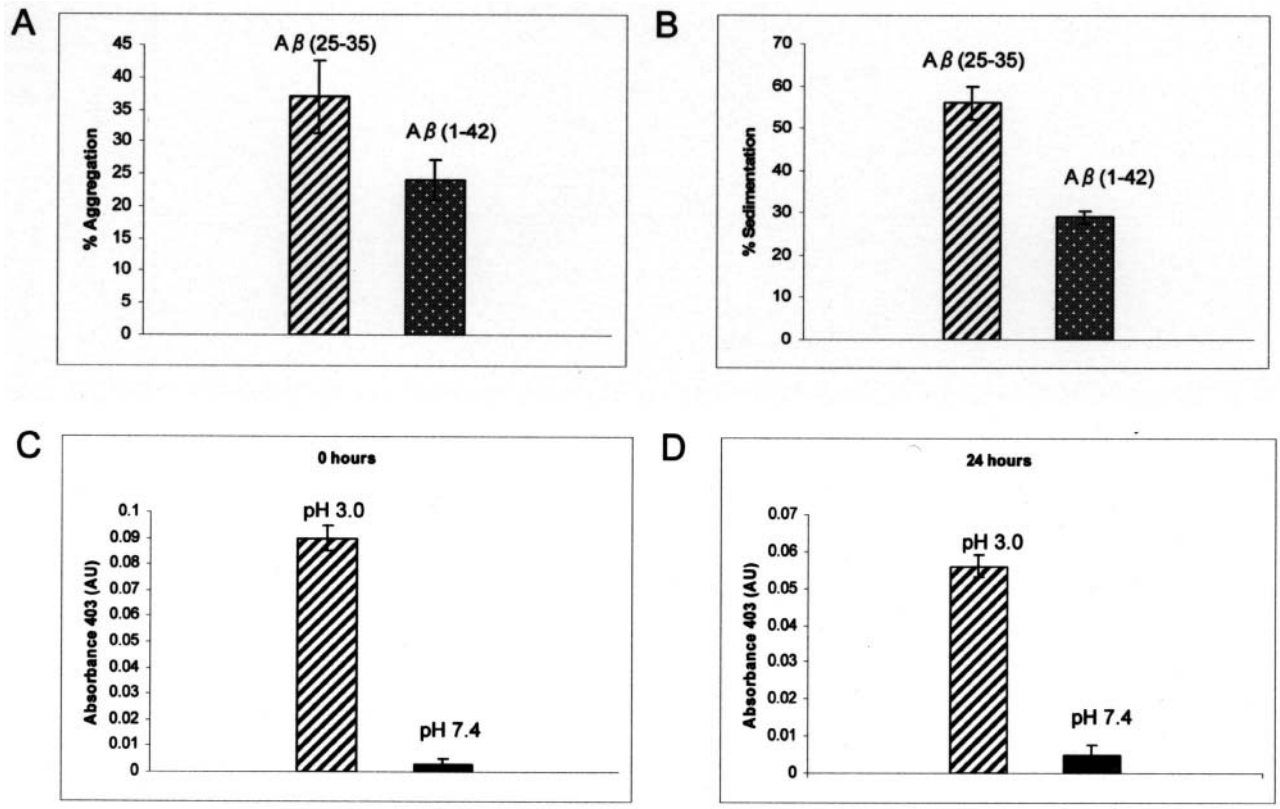

Figure 1. **(A)** UV OD_{220nm} spectroscopy assay. 10 μM Aβ(25-35) (pH 7.4) was incubated at 37°C for 30 min, and the percentage of total aggregation was calculated as described in Materials and Methods. The percentages of aggregation for Aβ(1-42) are also reported. **(B)** Sedimentation assay of Aβ(25-35) aggregation in H_2O. Aggregation of Aβ(25-35) was assessed by quantifying the percentage of peptide that had a sediment following 1 h of ultracentrifugation at 100 000 x g. The percentages of sedimentation for Aβ(1-42) are also reported. Results are the average of three independent experiments. Bars represent mean percentage sedimentation values. **(C, D)** Turbidity (*absorbance 403 AU*) at 0 (before pH shift) and 24 h (after pH shift) of: Aβ aggregates formed at pH 3 and shifted to pH 7.4 (left side), and Aβ aggregates formed at pH 7.4 and shifted to pH 3 (right side).

electrophoretic data, a strong tendency of Aβ(25-35) to aggregate, our findings are, to the best of our knowledge, the first experimental demonstration and a more exact quantification of such behaviour in H_2O.

We then quantitatively evaluated the kinetics of formation of Aβ(25-35) amyloid aggregates using the dye CR. Figure 2A shows the individual and combined spectral properties of aggregated Aβ(25-35) and CR in a solution at pH 7.4 at the start of the reaction, while figure 2C shows a shoulder peak at 541 nm formed during peptide aggregation. Absorbance spectra from 300 to 700 nm were recorded for the CR–Aβ mixture as well as for CR and Aβ alone; the Aβ + CR absorbance spectrum was appreciably greater than the spectral curve of CR alone; these spectra were used to determine the wavelength of absorbance of the CR–Aβ complex (541 nm) and the existence of a minimum point at 403 nm, common to CR alone and the CR–Aβ complex. Figure 2B shows the spectra at five different CR concentrations with the same amount of Aβ(25-35) (63 μg/ml); at 541 nm the change in absorbance spectrum resulting from CR binding to Aβ(25-35) aggregates was evident as a shoulder on the curve and was indicative of amyloid aggregation (Klunk *et al.* 1998). The shoulder peak remained constant at all CR concentrations and defined a suitable wavelength adopted for subsequent assays. When CR was bound to aggregated forms of Aβ(25-35), an appreciable change in colour from orange to pink was observed, corresponding to the shoulder peak in the characteristic absorbance spectrum of CR. Figure 2C shows the absorbance spectra at 541 nm at an interval of 30 s during the Aβ(25-35) aggregation process. At these spectra, absorbance gradually grew with time, indicating a kinetic bond between CR and amyloid aggregates, and suggesting that formation of the shoulder peak was firmly attributable to the aggregation of peptide.

To determine the exact aggregation time course of Aβ(25-35) in H_2O, we adopted a typical CR spectrophotometric assay. Depending on the parameters of synthesis and sample handling, preparations of commercial Aβ contain

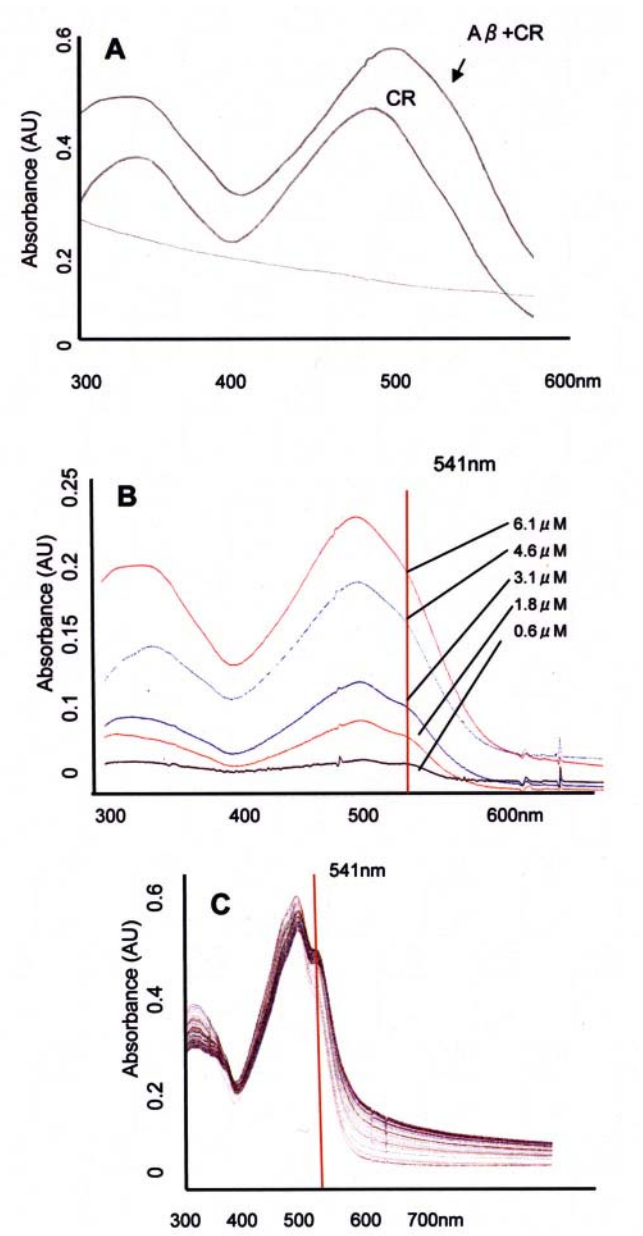

Figure 2. (A) Spectral features of Congo red (CR) and aggregated Aβ(25-35). Absorbance spectra of a suspension of 63 μg/ml Aβ(25-35) in the absence and presence of 6.2 μM CR and of CR alone. **(B)** Different absorbance spectra obtained at various concentrations of CR in the presence of 63 μg/ml Aβ. The change in absorption spectrum resulted from CR binding to aggregates. The spectra presented a shoulder peak at 541 nm due to the increase in absorbance owing to the turbidity of amyloid aggregates; note that the shoulder peaks at 541 nm were constant at all CR concentrations tested. **(C)** Relationship between the shoulder peak (541 nm) and time, for 45 μg/ml Aβ(25-35) in 20 mM CR. The peak change indicates a sigmoidal curve and the original absorbance spectra at 541 nm at intervals of 30 s on the aggregation of Aβ(25-35) are shown. The shoulder peaks at 541 nm gradually grew with time, indicating that CR is kinetically bound to the amyloid aggregates.

varying amounts of peptide that is chemically intact, but has undergone non-covalent aggregation. This implies that pre-existing aggregates may be originally present in commercial lots, thus preventing or even impairing an actual evaluation of aggregation kinetics. Consequently, if the aim is to monitor the actual modalities of Aβ aggregation, it is necessary to effectively purge the peptide sample from pre-existing aggregates. Usually, this is achieved by treatment with a solvent (TFA) capable of disaggregating these associated forms or by filtration to remove residual aggregates. Figure 3 shows the extent of aggregate formation as assessed by CR binding at different concentrations of Aβ(25-35) in a reaction at 25°C and in seeded conditions. As expected, the aggregation kinetics were sigmoidal, but the starting latency period was not appreciable. We found that the CR–peptide complex reached an OD maximum after only 4 min in a concentration-independent manner (figure 3). The reaction was initiated immediately upon mixing the peptide into the CR solution and a dose-dependent increase in absorbance was observed together with the addition of Aβ(25-35), starting with an Aβ-solution of 9 μg/ml and increasing the concentration up to 63 μg/ml. Once formed, the aggregates generated in H_2O at pH 7.4 were stable and resisted the disaggregating action of DMSO treatment (data not shown). In seeded conditions, Aβ(25-35) at pH 3 essentially showed the same behaviour as at pH 7.4, reaching maximum absorbance in 4 min but, in this case, the aggregates were unstable and subsequent treatment with DMSO was able to break them up (data not shown).

The rapid aggregation time of Aβ(25-35) in H_2O was further confirmed by the thiazole dye thioflavin-T (Th-T). This dye, when bound to proteins bearing the β-sheet structure, can be selectively excited to yield a fluorescent signal (Ban *et al.* 2003). The increase in Th-T fluorescence may precede the formation of precipitable complexes and is more sensitive than the use of CR. An increase in Th-T fluorescence is considered as an important indicator of the presence of amyloid fibrils (Eisert *et al.* 2006). So, to confirm the aggregation properties of Aβ(25-35) observed by CR, we monitored the changes in Th-T fluorescence intensity of Aβ(25-35) as a function of incubation time under stable environmental conditions (constant temperature, 25°C). Analysis of the fluorescent signal from the Th-T probe suggests that a significant proportion of the Aβ(25-35) peptide in H_2O was present in β-configuration since Th-T fluorescence was much more pronounced than when no peptide was used (figure 4A). The aggregation time of Aβ(25-35) shown by Th-T analysis was exactly in agreement with data obtained by CR experiments; however, there was a rapid decrease in Th-T fluorescence after reaching a maximum value, which was particularly appreciable at higher peptide concentrations. The fluorescence of Aβ(25-35)–Th-T bound at different concentrations showed a time course (figure 4A) suggesting nucleation-dependent fibril

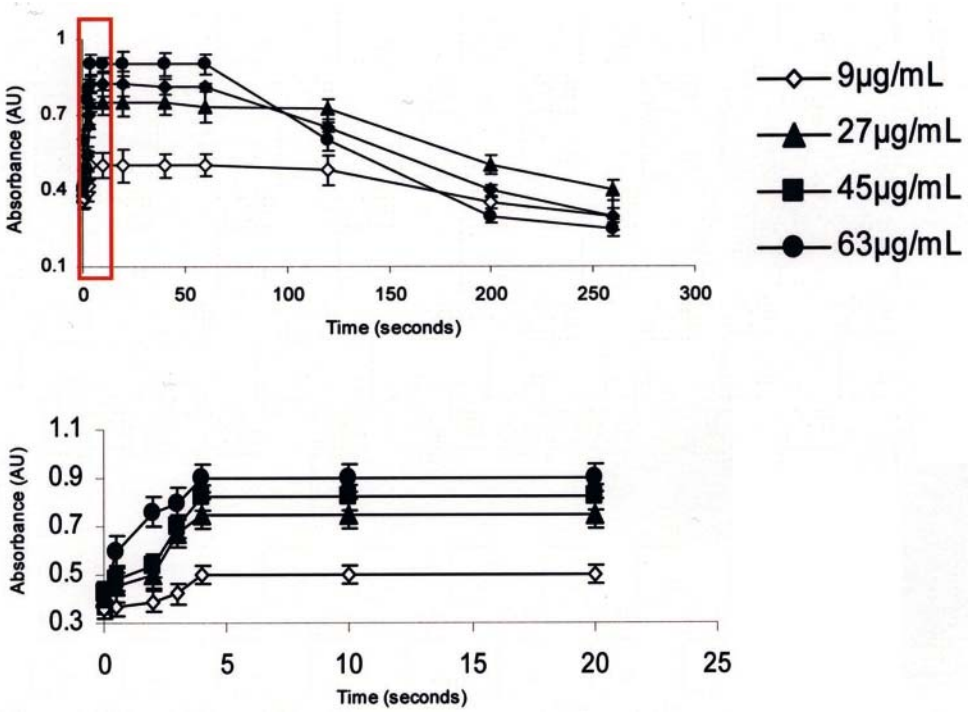

Figure 3. Kinetics of Aβ(25-35) aggregation in seeded conditions, resulting from the incubation in H_2O at pH 7.4. Different concentrations of Aβ(25-35) were mixed with 20 mM CR at pH 7.4 and incubated at room temperature. The absorbance spectra were recorded in kinetic mode at 403 nm and 541 nm until the complex CR–Aβ precipitated on the cuvette bottom. Lines represent kinetics of spontaneous Aβ(25-35) aggregation. The lower chart shows Aβ(25-35) aggregation kinetics during the first 4 min of monitoring. Results are the average of three independent experiments. Bars indicate standard deviations.

formation, but the lag phase was nearly completely lacking, maybe because Th-T interacted with Aβ(25-35) early in its aggregation pathway, i.e. at the nucleation or protofibril stage. The maximum value of fluorescence was then followed by a very rapid decrease. This behaviour was not congruent with the aggregation kinetics observed with CR.

It can be also emphasised that the observed aggregative ability of Aβ(25-35) was greater than that of the commonly studied Aβ(1-42) peptide. Comparatively, at around 4 min of observation, the aggregation of Aβ(25-35) reached a steady state, while the aggregation of Aβ(1-42), in the same seeded conditions, reached a steady state only after 3 h and 20 min (figure 4B).

Under unseeded conditions, Aβ(25-35) has an aggregation kinetic with an evident lag phase. Figure 5 shows the extent of aggregate formation as assessed by CR binding, at different pH; aggregate formation began within 60 min at pH 3.0 and reached completion in about 6 h. Also measured by CR, Aβ(25-35) began to aggregate after 3 h at pH 7.4 and was complete after about 5 h. To confirm data obtained from Aβ(25-35) observed by CR in unseeded conditions, we again observed the changes in Th-T fluorescence intensity of Aβ(25-35). Analysis of the fluorescent signal from the Th-T probe showed that, in this case, the aggregation time of Aβ(25-35) was exactly in agreement with data obtained by CR experiments (data not shown).

We also tested the differences between aggregation in stirred or unstirred conditions at pH 7.4 but this condition did not seem to influence the aggregation ability of peptide (data not shown).

Finally, we compared the abilities of aggregates generated at various pH to act as seeds for the initiation of fibril formation. We found that aggregates of Aβ(25-35) formed at pH 7.4 were able to stimulate fibril formation and reduce the lag time to achieve a complete aggregation reaction. In contrast, aggregates formed at pH 3.0 were unable to seed fibril formation when added to a solution at pH 7.4 (figure 5B). Thus, the aggregate suspension formed at pH 7.4 was functionally related to propagation of amyloid structure despite the turbidity generated by the aggregate at pH 3.

4. Discussion

This study is the first to provide information on the very rapid aggregation of Aβ(25-35) in water at pH 3.0 and pH 7.4. Due to to the adoption of suitable in-solution techniques and careful removal of undesirable pre-existing aggregation seeds, we were able to quantify the exact time necessary for

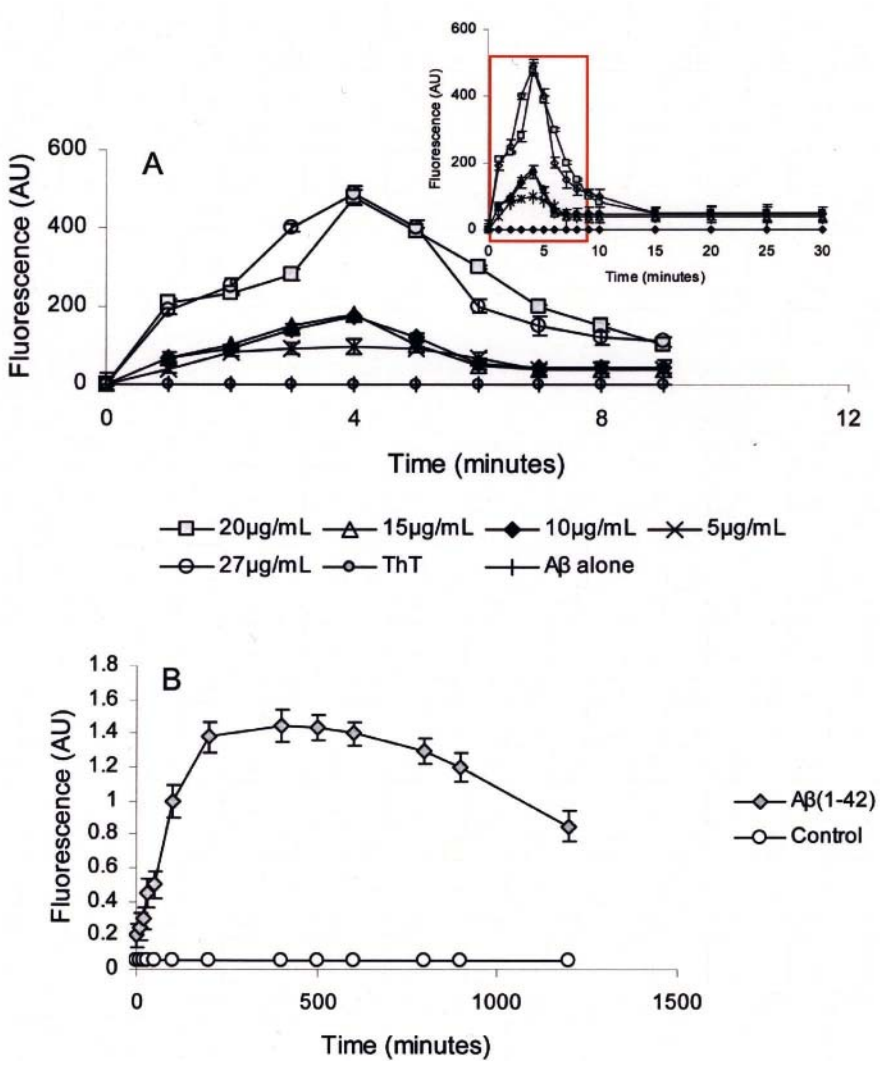

Figure 4. **(A)** Aggregation of Aβ(25-35) in seeded conditions, measured via Th-T fluorescence as a function of elapsed time of aggregation. The inset shows the aggregation of Aβ(25-35) during the first 10 min of the experiment. **(B)** Aggregation of 20 μg/ml Aβ(1-42) under the same conditions as Aβ(25-35). In both cases, data represent the mean Th-T fluorescence measurements of at least three independent experiments ($N \geq 3$). Bars indicate standard deviations.

the highly toxic Aβ(25-35) to self-assemble into stable and insoluble aggregated forms.

Several models for amyloid fibril formation have been suggested based on monitoring fibrillogenesis via microscopy, spectroscopic techniques and/or the binding of amyloid-specific dyes (Collins *et al.* 2004). As general rule, after the rate-limiting step of nucleus formation, growth of aggregates proceeds rapidly by further addition of monomers or other assembly-competent species. Whereas the formation of the nucleus is thermodynamically unfavourable, its subsequent elongation is highly favourable and proceeds rapidly to the ultimate fibril structure. By contrast, assembly of spherical oligomers and other prefibrillar forms occurs with nucleation-independent kinetics, and results in the formation of spherical particles. In the case of β_2m amyloid fibril formation, this has been extensively studied (Smith *et al.* 2006). While the incubation of native β_2m at pH 7 does not result in fibril formation in the absence of fibrillar seeds, incubating β_2m at pH values close to the isoelectric point (pI) results in the formation of amorphous aggregates, while at low pH values, worm-like fibrils (around pH 3.6) or long straight fibrils (around pH 2.5) are formed. These states represent thermodynamic ground states on the energy landscape. Assembly of β_2m into amyloid-like fibrils at low pH involves significant conformational rearrangement from the initially highly dynamic, unfolded monomer at very low pH (Platt *et al.* 2005) to the compact, stable cross-β structure of amyloid. In the case of Aβ(25-35), the peptide is able to aggregate at both neutral and acidic pH, but the aggregates show different properties. The aggregation kinetics of

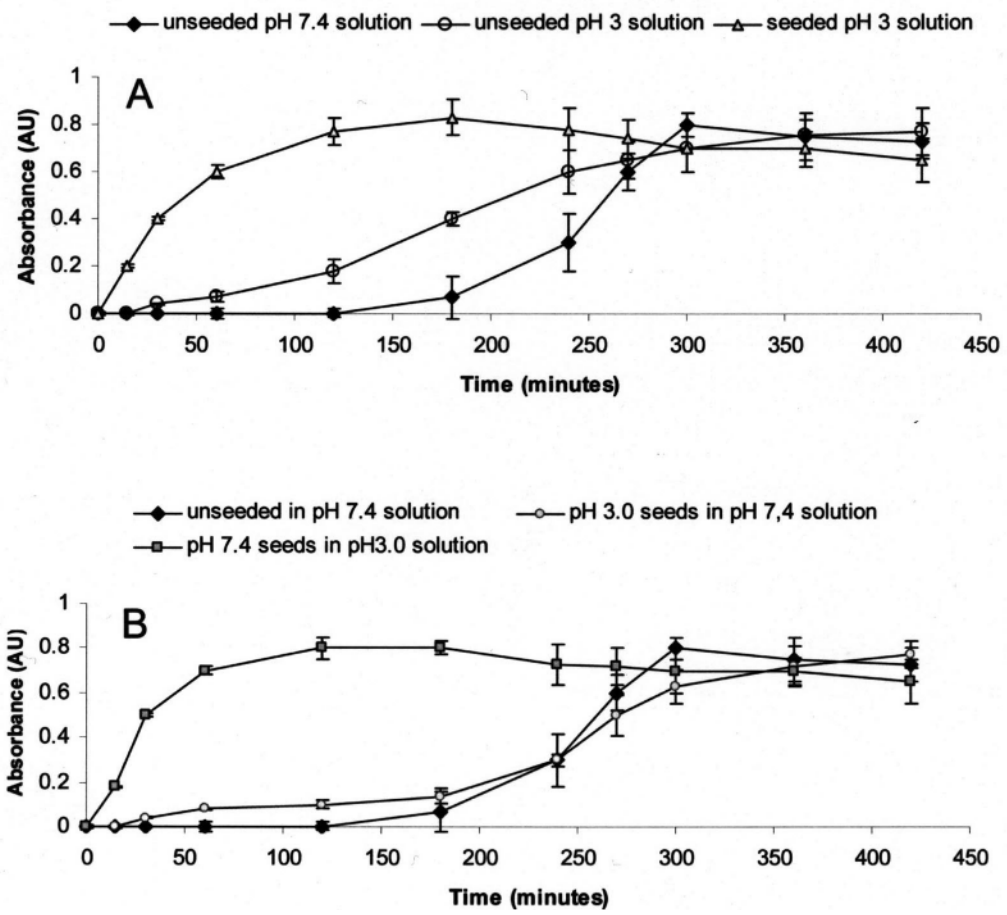

Figure 5. **(A)** Kinetics of aggregation of 63 μg/ml Aβ(25-35) in unseeded conditions, resulting from incubation in H_2O at pH 3.0 and at pH 7.4. Aβ(25-35) was mixed with 20 mM CR at pH 7.4 and incubated at room temperature. The absorbance spectra were recorded in kinetic mode at 403 nm and 541 nm until the complex CR–Aβ precipitated on the cuvette bottom. Lines represent the kinetics of spontaneous Aβ(25-35) aggregation. Kinetics of 63 μg/ml Aβ(25-35) aggregation made in seeded conditions at pH 3.0 is also presented to point out the difference between the seeded and unseeded conditions (*see also* figure 3 for Aβ(25-35) aggregation at pH 7.4 in seeded conditions). Data represent the mean absorbance measurements of at least three independent experiments ($N \geq 3$). Bars indicate standard deviations. **(B)** Seeding ability of various Aβ(25-35) aggregates. Reaction solutions of trifluoroacetic acid (TFA)-treated (*see* Materials and methods) Aβ(25-35) (63 μg/ml) in water (pH 7.4) at 25°C were seeded with 6.3 μg/ml (10% w/w) of Aβ fibrils previously formed at pH 3.0 from an unstirred pH 3.0 reaction (◻); equally, reaction solutions of TFA-treated Aβ(25-35) (63 μg/ml) in buffer (pH 3.0) at 25°C were seeded with 6.3 μg/ml (10% w/w) of Aβ fibrils previously formed at pH 7.4 from an unstirred pH 7.4 reaction (◆); the no added aggregate reaction of Aβ(25-35) in water at pH 7.4 is also shown to highlight the seeding efficiency of preformed aggregates (◆).

Aβ(25-35) shown by Th-T and CR experiments were in exact agreement but there was a rapid decrease in Th-T fluorescence after reaching a maximum value. Generally, the time course of fibril formation, as monitored by Th-T binding, follows a sigmoidal curve. The prefibrillar nuclei (early oligomeric species) do not bind Th-T. They form during the lag time which is followed by the fibril elongation phase corresponding to an increase in the dye's fluorescence. The subsequent plateau phase is associated with a decrease in the concentration of small species, or the aggregation and precipitation of fibrils (Ban *et al.* 2003). The time course of Th-T fluorescence upon interaction with Aβ(25-35) may reflect other processes in addition to the formation of amyloid fibrils. This may be due, at least partially, to the tendency of Aβ(25-35) to assemble in large conglomerates of tangled fibrils that may have a reduced Th-T-binding capacity, and this process is likely to be time-dependent at a set temperature (LeVine 1997), analogous to the temperature-induced 'precipitation' of insulin fibrils. The decrease in Th-T fluorescence over time after reaching a maximum may be also attributable to unstable fibrillar aggregation of Aβ(25-35), which might have reduced the number of fibrils in favour of amorphous aggregates. How the molecular characteristics of the precursor state and different kinetic routes influence the assembly reaction and ultimate fibril morphology will be the subject of future investigations. To this end, it may may

be important to point out that, according to the 'nucleated conformational conversion' (NCC) model of aggregate formation (Serio *et al.* 2000), a group of monomers initially present in solution coalesces to form 'molten' oligomers, which undergo a reorganisation process in succession and eventually give rise to more highly organized structures and fibrils rich in *β*-sheets. Thus, amyloid fibril formation is considered to be a consequence of the ability of the main chain of a protein to form hydrogen bonds; this property is common to all polypeptide chains and the competition between hydrophobicity and hydrogen bonding is a major determinant of the aggregation process. The hydrophobicity of the A*β*(25-35) peptide is not sufficient to drive an initial coalescence step, and the peptide can otherwise form ordered aggregates in a single step, driven by the formation of hydrogen bonds. This oligomerization of the A*β*(25-35) fragment, driven by hydrogen bond formation, may lead to oligomers with a small number of extended *β*-sheet structures. Evidence for the importance of the competition between hydrogen bonding and hydrophobic interactions in the aggregation process has been found in studies in which changes in solution conditions result in a change in the hydrogen bonding interactions and subsequently in aggregates with similar *β*-sheet content but with distinct morphological features (fibrillar or not) (Calamai 2005). By extension, the discrepancy observed in the present study between CR and Th-T experiments can also account for the observation of inherent structures of species formed prior to the mature fibrils. A basic understanding of the role of the initial solvent in determining the aggregation rate, extent and modality of A*β*(25-35) self-assembly will help to comprehend the pathway and key steps of A*β*(25-35) association.

The conditions in the brain are different from those in the *in vitro* experiment described here and the actual aggregation kinetics will differ. However, it is very likely that this amyloid fragment also aggregates rapidly in the brain, and that changes in the actual aggregation process could result in the formation of aggregated structures that may have powerful effects on synaptic activity. We cannot be entirely specific regarding the particular species involved in the toxicity, but this assumption derives from detailed biophysical studies aimed at identifying the formation of smaller oligomeric species at earlier stages of the amyloid aggregation process. Moreover, the significant toxicity of the early intermediates of A*β*(25-35) fibrils toward different kinds of cells (myoblasts, neurons, red blood cells) suggests that morphologically, it is the small oligomeric species rather than the large fibrillar aggregates that are toxic (Korczyn 2008).

Finally, the actual aggregation state would be another important variable affecting the results of neurodegenerative processes induced by *β*-amyloid fragments.

Acknowledgments

The authors worked like to thank Lorenzo Ghezzi and Lorenzo Ricci for technical assistance. LM was supported by a SienaBiotech fellowship. This work was partially supported by Fondazione Monte dei Paschi 2008 grants to AS.

References

Baglioni S, Casamenti F, Bucciantini M, Luheshi L M, Taddei N, Chiti F, Dobson C M and Stefani M 2006 Prefibrillar amyloid aggregates could be generic toxins in higher organisms; *J. Neurosci*. **26** 8160–8167

Ban J Y, Nguyen H T, Lee H J, Cho S O, Ju H S, Kim J Y, Bae K, Song K S and Seong Y H 2008 Neuroprotective properties of gallic acid from Sanguisorbae radix on amyloid beta protein (25-35)-induced toxicity in cultured rat cortical neurons; *Biol. Pharm. Bull*. **31** 149–153

Ban T, Hamada D, Hasegawa K, Naiki H and Goto Y 2003 Direct observation of amyloid fibril growth monitored by Th-T fluorescence; *J. Biol. Chem*. **278** 16462–16465

Bieschke J, Siegel SJ, Fu Y and Kelly JW 2008 Alzheimer's abeta peptides containing an isostructural backbone mutation afford distinct aggregate morphologies but analogous cytotoxicity. Evidence for a common low-abundance toxic structure(s); *Biochemistry* **47** 50–59

Bitan G and Teplow D B 2005 Preparation of aggregate-free, low molecular weight amyloid-beta for assembly and toxicity assays; *Methods Mol. Biol*. **299** 3–9

Bradford M M 1976 A rapid and sensitive method for the quantitation of microgram quantities of protein utilizing the principle of protein-dye binding; *Anal. Biochem*. **72** 248–254

Burdick D, Soreghan B, Kwon M, Kosmoski J, Knauer M, Henschen A, Yates J, Cotman C and Glabe C 1992 Assembly and aggregation properties of synthetic Alzheimer's A4/b amyloid peptide analogs; *J. Biol. Chem*. **267** 546–554

Calamai M, Chiti F and Dobson C M 2005 Amyloid fibril formation can proceed from different conformations of a partially unfolded protein; *Biophys. J*. **89** 4201–4210

Carrotta R, Manno M, Bulone D, Martorana V, and San Biagio P L 2005 Protofibril formation of amyloid *β*-protein at low pH via a non-cooperative elongation mechanism; *J. Biol. Chem.* **280** 30001–30008

Clementi M E, Marini S, Coletta M, Orsini F, Giardina B and Misiti F 2005 A*β*(31–35) and A*β*(25–35) fragments of amyloid *β*-protein induce cellular death through apoptotic signals: role of the redox state of methionine-35; *FEBS Lett*. **579** 2913–2918

Collins S R, Douglass A, Vale R D and Weissman J S 2004 Mechanism of prion propagation: amyloid growth occurs by monomer addition; *PLoS Biol*. **2** e321

Dobson C M 2006 Protein aggregation and its consequences for human disease; *Protein Pept. Lett.* **13** 219–227

D'Ursi A M, Armenante M R, Guerrini R, Salvadori S, Sorrentino G and Picone D 2004 Solution structure of amyloid beta-peptide (25-35) in different media; *J. Med. Chem*. **12** 4231–4238

Eisert R, Felau L and Brown L R 2006 Methods for enhancing the accuracy and reproducibility of Congo Red and Th-T assays; *Anal. Biochem*. **353** 144–146

Gazit E 2005 Mechanisms of amyloid fibril self-assembly and inhibition. Model short peptides as a key research tool; *FEBS J*. **272** 5971–5978

Hölscher C 2005 Development of beta-amyloid-induced neuro-degeneration in Alzheimer's disease and novel neuro-protective strategies; *Rev. Neurosci*. **16** 181–212

Holscher C, Gengler S, Gault V A, Harriott P and Mallot H A 2007 Soluble beta-amyloid(25-35) reversibly impairs hippocampal synaptic plasticity and spatial learning; *Eur. J. Pharmacol.* **561** 85–90

Jayaraman M, Kannayiram G and Rajadas J 2008 Amyloid toxicity in skeletal myoblasts: implications for inclusion-body myositis; *Arch. Biochem. Biophys*. **474** 15–21

Klunk W E, Pettegrew J V and Abrham D J 1998 Quantitative evaluation of Congo Red binding to amyloid-like proteins with a beta-pleated sheet conformation; *J. Histochem. Cytochem*. **37** 1273–1281

Korczyn A D 2008 The amyloid cascade hypothesis; *Alzheimers Dement*. **4** 176–178

Kubo T, Nishimura S, Kumagae Y and Kaneko Y 2002 In vivo conversion of racemized beta-amyloid ((D-Ser 26)A beta 1-40) to truncated and toxic fragments ((D-Ser 26)A beta 25-35/40) and fragment presence in the brains of Alzheimer's patients; *J. Neurosci. Res*. **70** 474–483

LeVine H 3rd 1997 Stopped-flow kinetics reveal multiple phase of Th-T binding to Alzheimer β(1-40) amyloid fibrils; *Arch. Biochem. Biophys*. **342** 306–316

LeVine H 2004 Alzheimer's beta-peptide oligomer formation at physiologic concentrations; *Anal. Biochem*. **335** 81–90

Maurice T, Lockhart B P and Privat A 1996 Amnesia induced in mice by centrally administered β-amyloid peptides involves cholinergic dysfunction; *Brain Res*. **706** 181

Meinke J H and Hansmann U H 2007 Aggregation of beta-amyloid fragments; *J. Chem. Phys.* **126** 014706

Misiti F, Sampaolese B, Pezzotti M, Marini S, Coletta M, Ceccarelli L, Giardina B and Clementi M E 2005 Aβ(31–35) peptide induces apoptosis in pc 12 cells: contrast with Aβ (25–35) peptide and examination of underlying mechanisms; *Neurochem. Int*. **46** 575–583

Nesgaard L, Vad B, Christiansen G and Otzen D 2009 Kinetic partitioning between aggregation and vesicle permeabilization by modified ADan; *Biochim. Biophys. Acta* **1794** 84–93

Petkova A T, Leapman R D, Guo Z, Yau W M, Mattson M P and Tycko R 2005 Self-propagating, molecular-level polymorphism in Alzheimer's beta-amyloid fibrils; *Science* **307** 262–265

Pike C J, Burdick D, Walencewicz A Z, Glabe C G and Cotman C W 1993 Neurodegeneration induced by beta-amyloid peptides in vitro: the role of peptide assembly state; *J. Neurosci*. **13** 1676–1687

Pike C J, Walencewicz-Wasserman A J, Kosmoski J, Cribbs D H, Glabe C G and Cotman C W 1995 Structure–activity analyses of β-amyloid peptides: contributions of the β 25–35 region to aggregation and neurotoxicity; *J. Neurochem*. **64** 253–265

Platt G W, McParland V J, Kalverda A P, Homans S W and Radford S E 2005 Dynamics in the unfolded state of beta2-microglobulin studied by NMR; *J. Mol. Biol*. **346** 279–294

Roychaudhuri R, Yang M, Hoshi M M and Teplow D B 2008 Amyloid beta-protein assembly and Alzheimer's disease; *J. Biol. Chem*. **8** 4749–4753

Serio T R, Cashikar A G, Kowal A S, Sawicki G J, Moslehi J J, Serpell L, Amsdorf M F and Lindquist S L 2000 Nucleated conformational conversion and the replication of conformational information by a prion determinant; *Science* **289** 1317–1321

Simmons L K, May P C, Tomaselli K J, Rydel R E, Fuson K S, Brigham E F, Wright S, Lieberburg I, Becker G W and Brems D N 1994 Secondary structure of amyloid beta peptide correlates with neurotoxic activity in vitro; *Mol. Pharmacol*. **45** 373–379

Smith A M, Jahn T R, Ashcroft A E and Radford S E 2006 Direct observation of oligomeric species formed in the early stages of amyloid fibril formation using electrospray ionisation mass spectrometry; *J. Mol. Biol*. **364** 9–19

Snyder S W, Ladror U S, Wade W S, Wang G T, Barrett L W, Matayoshi E D, Huffaker H J, Krafft G A and Holzman T F 1994 Amyloid-β aggregation: selective inhibition in mixtures of amyloid with different chain lengths; *Biophys. J*. **67** 1216–1228

Stefani M 2007 Generic cell dysfunction in neurodegenerative disorders: role of surfaces in early protein misfolding, aggregation, and aggregate cytotoxicity; *Neuroscientist* **13** 519–531

Takadera T, Sakura N, Mohri T and Hashimoto T 1993 Toxic effect of a beta-amyloid peptide (beta 22-35) on the hippocampal neuron and its prevention; *Neurosci. Lett*. **161** 41–44

Walsh D M and Selkoe D J 2004 Oligomers on the brain: the emerging role of soluble protein aggregates in neurodegeneration; *Protein Pept. Lett*. **11** 213–228

Wang S, Chang Y, Chen P and Liu K 2004 A kinetic study on the aggregation behavior of β-amyloid peptides in different initial solvent environments; *Biochem. Eng. J.* **29** 129–138

Wei G and Shea G E 2006 Effects of solvent on the structure of the Alzheimer amyloid-beta(25-35) peptide; *Biophys. J.* **91** 1638–1647

Wood S J, Maleeff B, Hart T and Wetzel R 1996 Physical, morphological and functional differences between pH 5.8 and 7.4 aggregates of the Alzheimers amyloid peptide Aβ; *J. Mol. Biol.* **256** 870–877

Yoshiike Y, Tanemura K, Murayama O, Akagi T, Murayama M, Sato S, Sun X, Tanaka N and Takashima A 2001 New insights on how metals disrupt amyloid beta-aggregation and their effects on amyloid-beta cytotoxicity; *J. Biol. Chem*. **276** 32293–32299

MS received 3 February 2009; accepted 29 April 2009

*e*Publication: 23 May 2009

Corresponding editor: AMIT CHATTOPADHYAY